wjert, 2018, Vol. 4, Issue 5, 299-316. *Original Article* ISSN 2454-695X

World Journal of Engineering Research and Technology
WJERT
www.wjert.org SJIF Impact Factor: 5.218

RESEARCH ON INDUSTRIAL ROBOT SERVO MOTOR CONTROLLING SPEED SENSORLESS ALGORITHM

Dr. Xinhua Yan*, Xinxing Yan and Kezhi Zhang

Nobot Intelligent Equipment (Shandong) Co., Ltd., Liaocheng, China 252000.

Article Received on 30/07/2018 **Article Revised on 20/08/2018** **Article Accepted on 10/09/2018**

***Corresponding Author**
Dr. Xinhua Yan
Nobot Intelligent Equipment (Shandong) Co., Ltd., Liaocheng, China 252000.

ABSTRACT

Permanent magnet synchronous motor is the most commonly applied motor for industrial robots. In this paper, the structure and working principle of permanent magnet synchronous motor are analyzed, and the mathematical model of permanent magnet synchronous motor in different coordinate system is introduced based on coordinate transformation. On this basis, the working principle of space voltage loss control algorithm for three-phase voltage source inverter is introduced, and the model of permanent magnet synchronous motor vector control system is set up. To realize the speed sensorless control of permanent magnet synchronous motor, the model reference adaptive algorithm is used to estimate the rotor speed and position, and the adaptive law is designed according to the theory of wave's super stability. Since the slow convergence rate of the traditional model referencing adaptive algorithm, the synovial state observer as an adjustable model is designed in this paper, and the corrective feedback closed-loop link is added in the state equation, which greatly improved the speed of the speed identification and realized the effective estimation of the position and speed of the motor. Finally, the hardware in loop simulation of the motor vector control is established by using MATLAB/Simulink. The simulation results show that the sliding mode variable structure MRAS speed observer proposed in this paper has good dynamic performance.

KEYWORDS: Permanent magnet synchronous motor; Vector control; MRAS sliding-mode; Dynamic speed estimator.

1. INTRODUCTION

With the rapid development of electronic power technology and microelectronics, permanent magnet synchronous motor has been widely used in different fields, such as agriculture, automobile industry, electric power industry and so on.[1,2] Compared with the traditional electromotor, Permanent magnet synchronous motor (PMSM) has the advantages of less loss, high efficiency and obvious power saving effect. Permanent magnet synchronous motor uses permanent magnets to provide excitation, simplifies the structure of the motor, reduces the cost of processing and assembly, and improves the reliability and efficiency of the motor operation. Therefore, permanent magnet synchronous moto has been widely used. Because the use of speed sensors will lead to increased cost, difficulty in installation, and low reliability, researchers have studied how to avoid using speed sensors in applications. They propose many control strategies for permanent magnet synchronous motor speed sensorless vector control system. The reference model based on the stator flux vector and the MRAS method of adjustable model are proposed in document.[3-5] The stator flux is calculated with voltage model and current model respectively. The adaptive algorithm is used to adjust the stator flux of the two models, and then the motor speed is measured. The disadvantage of this method is that the calculation is complex and the accuracy of the observer depends on the accuracy of the motor parameters, especially in the voltage model. The stator resistance varies with the temperature rise of the motor and has a great influence on the calculation results of the stator flux. In document,[6,7] a model reference adaptive method based on stator current is given. This method is simple and has good performance in middle and high speed. But the error of low speed running is large and the load is poor at less than 5% rated speed. It is only suitable for some situations where low speed operation is not high. In document,[8] the high frequency injection method of using the motor salient effect is used. This method needs to increase the extra bandpass filter, and the effect is obvious in the middle and low speed domain. But as the speed increases, the frequency of the high frequency injection current and the basic frequency current is getting closer and closer, and the resolution of the filter decreases and the estimation effect becomes worse. In order to obtain a better control algorithm, some researchers used the method of estimating the rotor position, including the back EMF integral method,[9,10] the model reference adaptive,[11] the extended Kalman filter method,[12] the sliding mode variable structure observer[13,14] and so on. The inverse electric integral method is easily affected by the change of motor parameters, and there is a constant drift of the stator flux integral. The model referencing adaptive method is simple, but sensitive to the change of the parameters; the extended Kalman filter method has large real-time computation, high dependence on the control chip, and the dynamic response is not ideal. The sliding mode observer has the characteristics of fast response, insensitivity to system internal parameter changes and external disturbances, and is simple and easy to implement. However, this kind of sensorless detection method based on the back electric or state observer is only suitable for high speed. At low speed, the position estimation precision is reduced due to the inability to obtain enough phase voltage or back EMF. Therefore, in the start-up stage of motor, a different position sensorless control strategy is needed.

In this paper, the model referencing adaptive principle is used to select the output of half back EMF for the same physical meaning, and the speed and position signals are extracted by adaptive control law. Under the above guidance, an adaptive variable structure sliding mode observer for extended state of permanent magnet synchronous motor is proposed. The extended state adaptive sliding mode observer is constructed with stator current and half reverse potential. The adaptive speed adaptive law is proposed by using the equivalent semi reverse EMF and the estimated semi reverse EMF model reference self-adaptive system. The output of the adjustable model is close to the output of the reference model, thus the speed signal and the half reverse EMF estimation signal of the permanent magnet synchronous motor are extracted, and the system buffeting is weakened when the traditional sliding mode observer is calculated to get the position and speed signal. According to Lyapunov's improved pulse vibration high frequency injection method, it is based on the traditional pulse vibration high frequency injection method. It simplifies the dynamic performance of the motor at the low speed section and makes it easy to do in the process of current signal processing. The model referencing adaptive law varies with the difference between the reference model and the adjustable model. The rotor speed and position estimation can be obtained by the adaptive law. Finally, the stability of the control method is proved under the Popov super stability theory. Finally, a motor model based on variable structure sliding mode observer and model referencing adaptive motor model is built, and the simulation analysis is carried out.

2. Mathematical model of permanent magnet synchronous motor

2.1 Coordinate transformation of space vector

The coordinate transformation of space vector is an important mathematical method to simplify the complex model of permanent magnet synchronous motor, and is the foundation of vector control for permanent magnet synchronous motor. The coordinate transformation of space vector mainly refers to the *ABC* transformation between three stationary coordinate systems, $\alpha\beta$ two stationary coordinate systems and *d-q* two rotating coordinate systems. The motor stator currents in these three coordinate systems are shown in Figure 1.

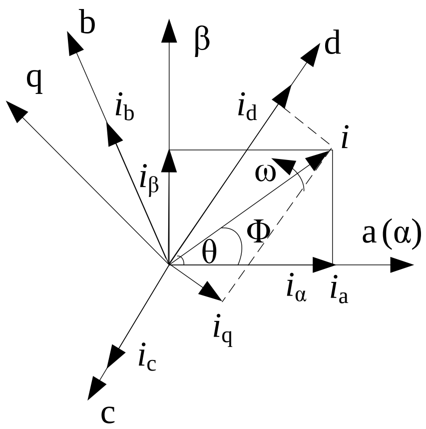

Figure 1: Stator current diagram in three coordinate systems.

It is shown that in the *ABC* three stationary coordinates, the *ABC* three axis angle difference is 120 degrees, the stator three-phase i_a, i_b and i_c current is equal in size, which is located on the *a*, *b*, and *c* three axes respectively. The current vector is i, and the rotational speed of the rotating magnetic field is ω. In the $\alpha\beta$ two phase stationary coordinate system, the positive direction of α axis coincides with the positive direction of an axis. The α axis lags behind the β axis ninety electric angles in space, the current vector i and the α axis are positive angle of φ, and the current component on the α and the β axis is i_α and i_β respectively. In the *d-q* two phase rotating coordinate system, the direction of d axis is consistent with the direction of the rotor flux, lagging behind the electric angle of the *q* axis at 90 degrees in space, and the whole coordinate system rotates in space at the synchronous speed ω_e, the angle of the current vector *i* and the *d* axis is θ, and the components decomposed to the *d-q* axis are i_d and i_q respectively. In order to realize the transformation between the three coordinate systems, two coordinate transformation methods are needed, namely, the *Clark* transformation between the three-phase stationary coordinate system and the two-phase stationary coordinate system, and the *Park* transformation between the two-phase stationary coordinate system and the two-phase synchronous rotating coordinate system. *Clark* transformation can be introduced from Figure 1.

$$\begin{cases} i_\alpha = i_\alpha - i_b \sin 30° - i_c \sin 30° \\ i_\beta = 0 + i_b \cos 30° - i_c \cos 30° \end{cases} \tag{1}$$

Form the form of a matrix

$$\begin{bmatrix} i_\alpha \\ i_\beta \end{bmatrix} = \sqrt{\frac{2}{3}} \begin{bmatrix} 1 & -0.5 & -0.5 \\ 0 & \sqrt{\frac{3}{2}} & \sqrt{\frac{3}{2}} \end{bmatrix} \begin{bmatrix} i_a \\ i_b \\ i_c \end{bmatrix} \tag{2}$$

Clark inverse transform

$$\begin{bmatrix} i_a \\ i_b \\ i_c \end{bmatrix} = \sqrt{\frac{2}{3}} \begin{bmatrix} 1 & 0 \\ -0.5 & \sqrt{\frac{3}{2}} \\ -0.5 & \sqrt{\frac{3}{2}} \end{bmatrix} \begin{bmatrix} i_\alpha \\ i_\beta \end{bmatrix} \tag{3}$$

From Figure 1, the *Park* transformation is introduced

$$\begin{cases} i_d = i_\alpha \cos\theta + i_\beta \sin\theta \\ i_q = -i_\alpha \sin\theta + i_\beta \cos\theta \end{cases} \tag{4}$$

The form of a matrix is the form of a matrix

$$\begin{bmatrix} i_d \\ i_q \end{bmatrix} = \begin{bmatrix} \cos\theta & -\sin\theta \\ \sin\theta & \cos\theta \end{bmatrix} \begin{bmatrix} i_\alpha \\ i_\beta \end{bmatrix} \tag{5}$$

Park inverse transform array

$$\begin{bmatrix} i_\alpha \\ i_\beta \end{bmatrix} = \begin{bmatrix} \cos\theta & -\sin\theta \\ \sin\theta & \cos\theta \end{bmatrix} \begin{bmatrix} i_d \\ i_q \end{bmatrix} \tag{6}$$

2.2 The mathematical model of permanent magnet synchronous motor

The mathematical model of permanent magnet synchronous motor is composed of stator voltage equation, flux linkage equation, torque equation and mechanical motion equation. Because permanent magnet synchronous motor is a nonlinear complex system, it is difficult to establish a precise mathematical model.[15] Therefore, to simplify the model analysis process, we often neglect some parameters with less influence. Therefore, the following assumptions are made before establishing the mathematical model of PMSM.[16]

(1) The stator armature winding produces sinusoidal induction electromotive force, and the air gap magnetic field of the rotor permanent magnet is also distributed in the air gap space with sine wave;

(2) The eddy current and hysteresis losses of stator and rotor cores are negligible;

(3) The saturation of the stator core is negligible and the inductance parameters remain unchanged. And it is considered that the magnetic path is linear；

(4) Neglecting the damped windings of the rotor.

The voltage equation and flux linkage equation of motor stator winding are not constant coefficient equations, but strong coupling time-varying equations. After decoupling the motor, the voltage equation and flux linkage equation of the stator winding of the motor are converted to solving the easier constant coefficient equation. The expression of the voltage equation after its transformation:

$$\begin{cases} u_d = R_s \cdot i_d + L_d \cdot pi_d - \omega_e \cdot L_q \cdot i_q \\ u_q = R_s \cdot i_q + L_q \cdot pi_q - \omega_e \cdot L_q \cdot i_q + \omega_e \cdot \psi_f \end{cases} \tag{7}$$

The u_d and u_q denote the stator voltage in the *d-q* coordinate system in the equation; i_d and i_q represent the stator current in the *d-q* coordinate system; *L* represents the equivalent number of inductance in the *d-q* coordinate system; R_s represents the stator resistance; ω_e represents the angular velocity of the motor rotor; the stator flux ψ_s of the motor is composed of the full flux linkage ψ_a , ψ_b and ψ_c in the static three phase *ABC* shaft system; The rotor chain ψ_f consists of ψ_{fa} , ψ_{fb} , and ψ_{fc} . Its motor flux linkage equation:

$$\psi_s = L_s i_s + \psi_f \tag{8}$$

For permanent magnet synchronous motor , the *d* axis of *d-q* two phase synchronous rotating coordinate system coincides with the axis of rotor pole, and the *q* axis converse clockwise forward d axis 90 electric angle, the angle of the axis of d axis and the stator winding of A phase of motor is θ_e , and rotate with the angular velocity ω_e of the rotor in space. ABC three phase stationary coordinate system and *d-q* two-phase synchronous rotating coordinate system is shown in Figure 2.

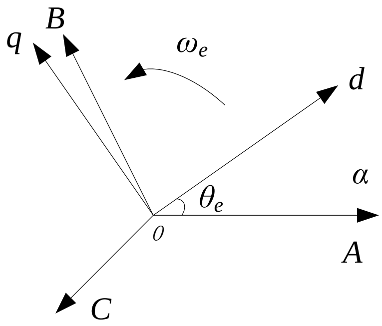

Figure 2: Three phase stationary coordinate system and two phase synchronous rotating coordinate system.

The flux linkage equation of PMSM in *ABC* three-phase stationary coordinate system is decomposed into the flux linkage equation in *d-q* coordinate system.

$$\begin{cases} \psi_f = L_d \cdot i_d + \psi_f \\ \psi_q = L_q \cdot i_q \end{cases} \tag{9}$$

where ψ_f is the flux linkage between rotor permanent magnet and stator winding; L_d and L_q are direct reactance and cross axis reactance; i_a , i_b and i_c are three-phase stator currents of permanent magnet synchronous motor; ψ_a , ψ_b and ψ_c are three-phase stator flux linkage of permanent magnet synchronous motor.

Electromagnetic torque equation of motor

$$T_e = \frac{3}{2} n_p .(\psi_d .i_q - \psi_q .i_d) \tag{10}$$

Combination Eq. 4 and Eq. 6

$$T_e = \frac{3}{2} n_p \left[\psi_f i_q + (L_d - L_q)) \right] .i_q .i_d) \tag{11}$$

The equilibrium expression of the mechanical motion balance equation for three phase permanent magnet synchronous motor is as follow

$$J \cdot \frac{d^2\theta_r}{d^2 t} + D \cdot \frac{d\theta_r}{dt} + K \cdot \theta_r = T_e - T_L \tag{12}$$

where θ_r is the mechanical angle; the T_L is the load torque; the J is the moment of inertia; the D is the friction and the wind resistance torque coefficient which is proportional to the speed, and the K is the torsion elastic torque coefficient.

In general, K can be approximately equal to zero, Load torque T_L can be incorporated into the frictional resistance moment, Thus, the dynamic equation of calculation is simpler, that is

$$\frac{J}{n_p} \cdot \frac{d\omega_e}{dt} = T_e - T_L \quad (13)$$

3. The principle and Realization of vector control

For the three-phase permanent magnet synchronous motor, the voltage, current, magnetic potential and magnetic chain of the fixed rotor are rotated at the synchronous speed in space, and their components on the three-phase stationary coordinate axis are all inflow, and it is inconvenient to calculate, adjust and control them directly. And through vector control, the stator three phase current i_a, i_b and i_c of the motor are transformed from three-phase stationary coordinate system to DC current i_d and i_q of two phase rotating coordinate system. In this way, the exchange physical quantities are transformed into DC physical quantities. It can be seen from Eq. 10 that the excitation and flux linkage of the permanent magnet is determined by the permanent magnet itself, and the inductance of the motor stator is also the parameter of the motor itself. In this way, the torque component i_q and the excitation component i_d of the stator current determine the torque of the motor; i_d and i_q are equivalent to the excitation current and torque current in the DC motor. By controlling the two current of i_d and i_q, the permanent magnet synchronous motor can be controlled like the DC motor.

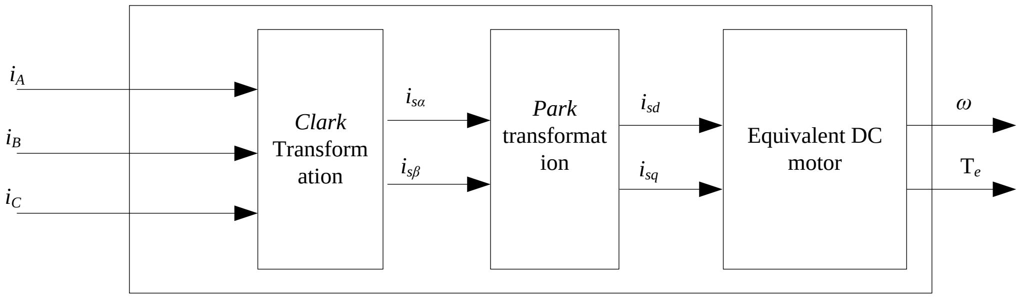

Figure 3: Bit vector control schematic diagram.

In the Eq.9, if $i_d=0$, the stator current vector i_s, only *q* axis component, no *d* axis component. There is an electromagnetic torque equation.

$$T_e = \frac{3}{2} n_p . \left[\psi_f . i_q + (L_d - L_q)) \right] . i_q . i_d \quad (14)$$

It can be seen from the formula that the alternating and direct axis currents in the torque expressions are completely decoupled, and because of the permanent magnet rotor, ψ_f is a constant value. Therefore, the electromagnetic torque is proportional to the *q* axis component i_q of the stator current and can achieve the same control effect as DC motor. At this point, the torque to current ratio is the largest, and the minimum stator current can be used to generate the required torque. Moreover, due to the decrease of stator current, copper consumption is reduced and motor efficiency is improved. As shown in Figure 4, the block diagram of vector control system using $i_d=0$ control mode is presented. The whole control system mainly includes permanent magnet synchronous motor, PI controller module, Park inverter module, voltage space vector pulse width modulation module (SVPWM), three-phase full bridge inverter circuit, stator current acquisition module, rotor position acquisition module, *Clark* transform module, *Park* transform module, and flux observer module.

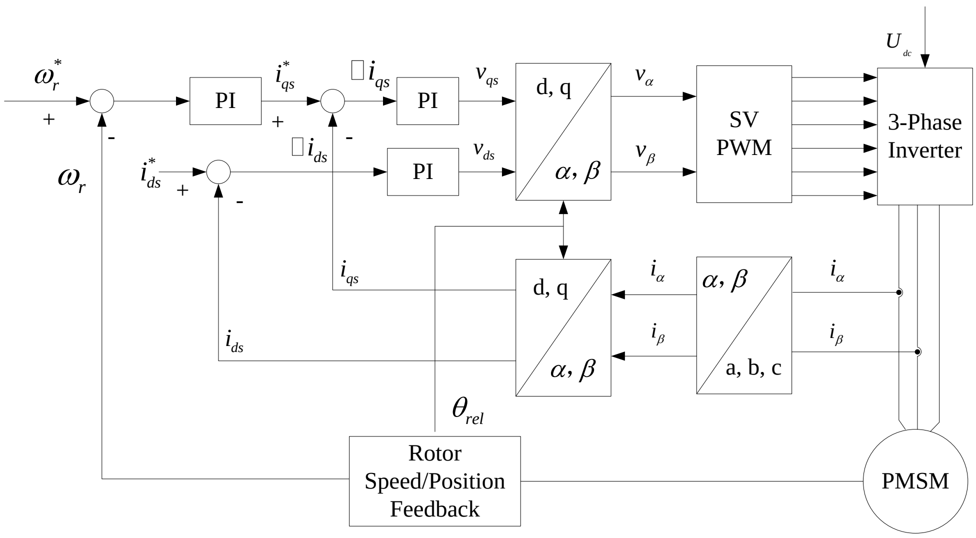

Figure 4: Vector control diagram of permanent magnet synchronous motor.

The vector control system is divided into two negative feedback loops, the outer ring is the speed loop, which ensures the actual speed of the motor to track the given speed steadily, and the inner ring is the current loop, which ensures the fast and stable current of the motor to track the given current.[17-18]

The stator current i_a, i_b and i_c under the three-phase stationary coordinate system collected by the current sense sensor are transformed into i_d and i_q in the $\alpha\beta$ two phase stationary coordinate system by Clark. Because i_d and i_q are DC components, the permanent magnet synchronous motor can be controlled by controlling these two currents. The difference between i_d and i_q are the corresponding expected excitation current i_d^* and torque current i_q^* are the input of the current PI controller. The PI controller outputs the desired d axis control voltage u_d and the desired q axis control voltage u_q, and then through inverse *Park* transform, the α axis component u_α and β axis component u_β of the stator voltage in the $\alpha\beta$ biphasic stationary coordinate system are obtained; u_α and u_β are modulated by SVPWM module and output six PWM waves. It is used to control six switch tubes in the three-phase full bridge inverter circuit, and output the three-phase AC voltage to the permanent magnet synchronous motor and complete the inner loop current control. For the speed outer loop, as shown in Figure 4, the desired torque current i_q^* required for the current inner loop control is given by the PI speed controller in the speed outer loop control. The input speed of the PI speed controller is the difference between the expected speed ω_m^* and the mechanical speed ω_m. The mechanical speed ω_m is calculated by collecting the rotor position information of the speed sensor. In the block diagram above, the θ parameters of the *Park* transform and the *Park* inverse transform module are obtained by integrating the actual speed of the flux observer module.

4. Speed sensorless technology

In the modern AC speed regulation system, in order to get high performance speed control, speed closed-loop control is adopted, and speed sensors must be installed on the motor shaft. But in practical systems, the installation of speed sensors is often limited. The main problems are the following problems.

(1) The installation of speed sensor reduces the robustness and simplicity of the system.

(2) High precision speed sensors generally cost more and increase system costs.

(3) In some harsh conditions, such as high temperature, humidity, etc., the installation of speed sensors will reduce the reliability of the system.

(4) There are some difficulties in the installation of speed sensors. If they are not installed properly, they will become a fault source of the system.

In order to avoid these problems, people turn to study speed identification methods without speed sensors. In recent years, this research has become a hot issue in AC drive. Foreign studies began in 1970s. For the first time, the application of speed sensorless to vector control was completed in 1983 by *R. Joetten*, which made the development of AC drive technology a new step. In the following ten years, scholars at home and abroad have done a lot of work in this field, and so far, many methods have been put forward. In general, these methods can be divided into the following: ①Dynamic speed estimator; ②Model reference adaptive (MRAS); ③Based on PI regulator method; ④Adaptive speed observer; ⑤Rotor tooth harmonic method; ⑥High frequency injection method; ⑦A method based on artificial neural network. In a variety of different methods, model reference adaptive system is the most popular technique. If the speed deduction is attributed to reference identification, the model reference adaptive theory (MRAS) can be used to construct a system that can identify speed. In this case, the system is a nonlinear system, so the super stability theory of Popov can be used to deduce the identification algorithm under the condition of ensuring the stability of the system.

In all kinds of observers, sliding mode variable structure is not very demanding for the precision of the mathematical model of the system. It is not sensitive to the change of the system parameters and the disturbance of the external disturbance, and the control method is simple and easy to be realized. It gets the universal attention of the scholars at home and abroad and has been widely used in the field of electric drive. But because the uncertain factors such as variable structure control meet the "matching condition", that is, "matching condition", that is, it has the robustness against external interference and internal parameter perturbation, but it is difficult to determine the upper and lower bounds of the change of the uncertain parameters in practice. Therefore, the boundary of uncertain factors can be estimated in real time by using the adaptability of MRAS to the change of system parameters, and a variable structure MRAS speed identification algorithm is proposed. In this method, the variable structure control has the robustness against external interference and internal parameter perturbations and the adaptability of MRAS to the change of system parameters. This method can achieve accurate and rapid tracking of the reference model, meet the requirements of the system steady-state error, improve the accuracy of the magnetic chain observation, and then improve the precision of the speed identification Degree.

4.1 Construction of state error equation

According to the voltage equation flux linkage equation of AC induction motor in two-phases stationary $\alpha\beta$ coordinate system, the rotor flux linkage voltage model under two-phases stationary $\alpha\beta$ coordinates is established.

$$\begin{cases} \psi_{ra} = \frac{L_r}{L_m}\left[\int\left(u_{s\alpha} - R_s i_{s\alpha}\right)dt - \sigma L_s i_{s\alpha}\right] \\ \psi_{r\beta} = \frac{L_r}{L_m}\left[\int\left(u_{s\beta} - R_s i_{s\beta}\right)dt - \sigma L_s i_{s\beta}\right] \end{cases} \tag{15}$$

According to the state equation of AC induction motor in two phase stationary $\alpha\beta$ coordinate system, the rotor flux linkage current model in two phase stationary $\alpha\beta$ coordinate system can be obtained.

$$\frac{\mathrm{d}}{\mathrm{dt}}\begin{bmatrix}\psi_{ra}\\ \psi_{r\beta}\end{bmatrix} = A_r\begin{bmatrix}\psi_{ra}\\ \psi_{r\beta}\end{bmatrix} + b\begin{bmatrix}i_{s\alpha}\\ i_{s\beta}\end{bmatrix} \tag{16}$$

where $A_r = \begin{bmatrix} -\frac{1}{T_r} & -\omega \\ \omega & -\frac{1}{T_r}\end{bmatrix}$, $b = -\frac{L_m}{T_r}$.

As the rotor speed information is included in the current model, the model is selected as an adjustable model, and the rotor flux voltage model is employed as a reference model, and Eq. 16 is simplified

$$\frac{\mathrm{d}}{\mathrm{dt}}\psi_r = A_r\psi_{ra} + bi_{s\alpha} \tag{17}$$

The rotor flux estimation model with adjustable parameters is constructed.

$$\frac{\mathrm{d}}{\mathrm{dt}}\begin{bmatrix}\hat{\Psi}_{r\alpha}\\ \hat{\Psi}_{r\beta}\end{bmatrix} = \hat{A}_r\begin{bmatrix}\hat{\Psi}_{r\alpha}\\ \hat{\Psi}_{r\beta}\end{bmatrix} + b\begin{bmatrix}i_{s\alpha}\\ i_{s\beta}\end{bmatrix} \tag{18}$$

where $\hat{A}_r = \begin{bmatrix} -\frac{1}{T_r} & -\hat{\omega} \\ \hat{\omega} & -\frac{1}{T_r}\end{bmatrix}$, $\hat{\Psi}_{r\alpha}$ and $\hat{\Psi}_{r\beta}$ are the estimated values of rotor flux components respectively, and *W* is the estimated value of rotor angular velocity.

The Eq.19 is simply written as

$$\frac{\mathrm{d}}{\mathrm{dt}}\hat{\Psi}_r = \hat{A}_r\hat{\Psi}_r + bi_s \tag{19}$$

Definition of error state

$$e_\psi = \hat{\Psi}_r - \Psi r \tag{20}$$

The error equation of Eq.19 subtraction Eq. 20.

$$\frac{\mathrm{d}}{\mathrm{dt}}e_\psi = A_r\Psi_r - \hat{\Psi}_r(\hat{\omega} - \omega) \tag{21}$$

4.2 Switching function construction

The principle of selecting switching surfaces is that s(e) =0 occurs when the system slips, and the sliding motion is asymptotically stable and has better dynamic quality. According to this principle, the switching functions of the variable structure MRAS speed identifier constructed are as follows.

$$s = \Psi_{r\beta}\hat{\Psi}_{r\alpha} - \Psi_{r\alpha}\hat{\Psi}_{r\beta} \tag{22}$$

4.3 Determination of the equivalent velocity

According to the basic idea of variable structure control, if the system enters sliding mode control, then S=0. The expression of the equivalent velocity is as follows

$$\omega_{eq} = \omega + \frac{L_m i_{sa}(\Psi_{r\beta} - \hat{\Psi}_{r\beta}) + L_m i_{s\beta}(\hat{\Psi}_{r\alpha} - \Psi_{r\alpha})}{T_r(\hat{\Psi}_{r\alpha}\Psi_{r\alpha} + \hat{\Psi}_{r\beta}\Psi_{r\beta})} \tag{23}$$

This formula shows that when the estimated flux is convergent to the reference flux, the equivalent velocity converges to the real velocity.

4.4 Design of sliding mode observer

According to the obtained switching function and equivalent speed, the speed observer can be designed. When the constant switching control method is adopted, the speed estimation expression is as follows:

$$\hat{\omega} = M\,\mathrm{sgn}(s) \tag{24}$$

where M is a constant greater than zero; $\mathrm{sgn}(s)$ is a sign function. This formula shows that the velocity; $\hat{\omega}$ is a discrete function of the switching function, and its low frequency component is the equivalent velocity. In order to weaken the buffeting, the filter method is used. The low-pass filter is used to smooth the control signal and weaken chattering effectively.

5. Build a simulation model

5.1 Build a motor model

According to the voltage equation of the permanent magnet synchronous motor in the *d-q* shafting, the motor model in two phase stationary coordinate system is built as follows.

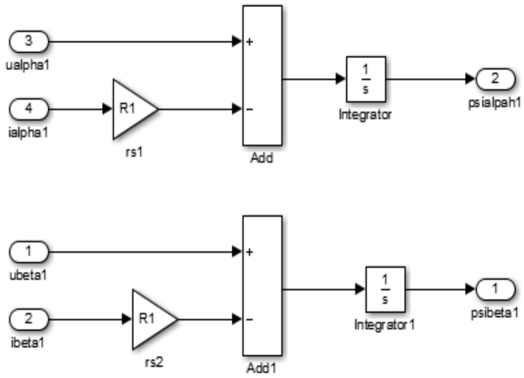

Figure 5: Motor model.

5.2 Construction of vector control system

According to the principle of vector controller, the following vector control system is built.

Speed PI control module:

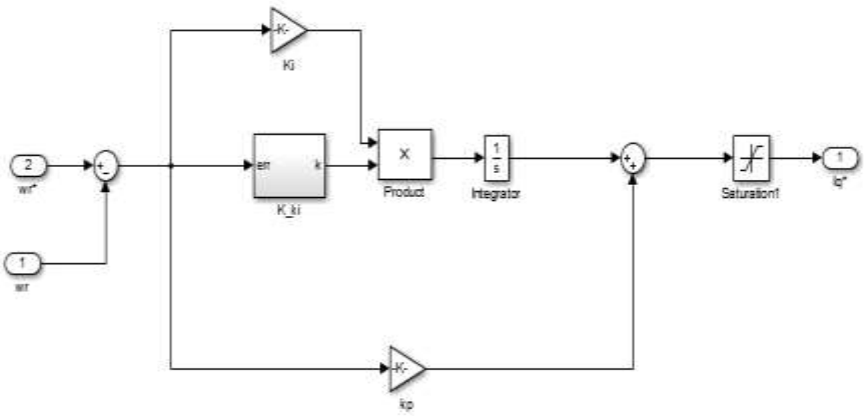

Figure 6 Speed PI control module.

5.3 Construction of sliding mode observer module

A sliding mode observer with variable structure is built according to the principle and formula of sliding mode observer.

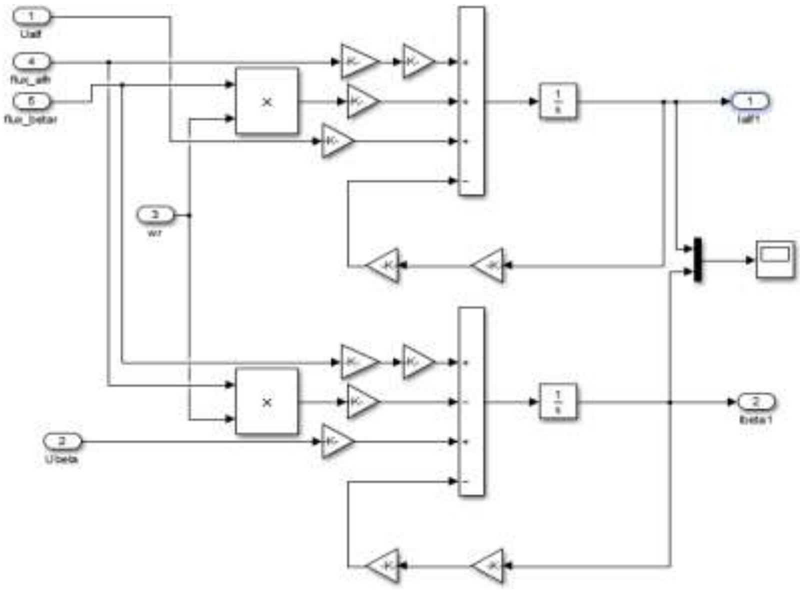

Figure 7: Current estimation module.

6. Simulation results and comparison

In the estimation formula of rotor speed, the selection of *M* value has a great influence on the performance of the speed regulating system. Generally speaking, the larger the M value is chosen, the better the control of sliding mode variable structure is, but at the same time, it will bring more obvious buffeting phenomenon. When the *M* value is reduced, the chattering phenomenon is obviously improved, but if the *M* value is too small, the speed regulation system cannot work normally.

Figure 8 is the speed and flux linkage curve when the speed is abrupt. The horizontal axis is in seconds, and the vertical axis is rpm. The given load is 10 N/m, and the given speed is 1200 rpm. It can be seen from the diagram that the rotational speed of the measurement module is smooth and the tracking performance is good in the steady state. The calculated speed is swinging back and forth along the sliding surface in a small range, and the difference is very small. It shows that the speed estimation method can reflect the rotor speed of the motor in time. After 0.5 seconds, the motor will reenter the steady state and have no overshoot. It shows that this speed regulation method has better dynamic performance and can meet the general engineering requirements, but there is a certain speed fluctuation phenomenon after steady state.

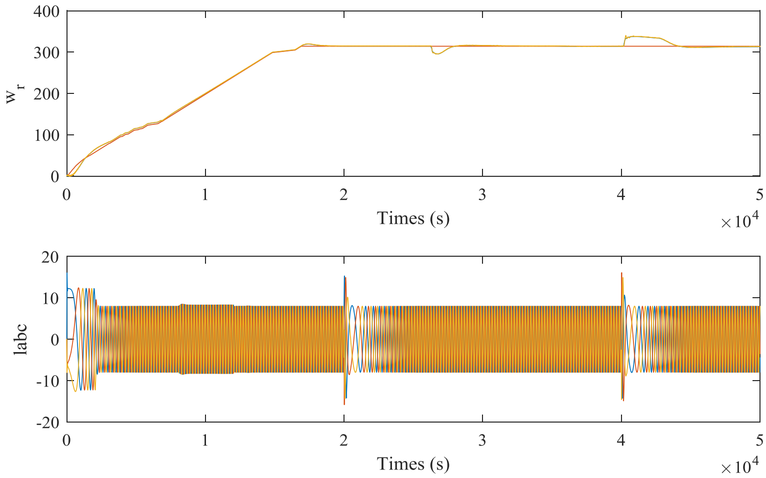

Figure 8: Speed and magnetic chain curve when the speed is abrupt.

Figure 9 shows the change of state when the motor runs steadily at 1.5R; rated load at 300 r/min. When the load is suddenly increased, the running speed of the motor drops to 50 r/min, and the torque drops rapidly. After the motor running speed begins to recover from the lowest point, the output torque is basically stable. When the load is added to the motor, the speed of the motor is restored to the stable running value. The time is about 0.5s. It can be seen from the actual speed wave and current waveform that the motor runs very stable with the rated load of 1.5 times. The experiment shows that when the given speed is 300 r/min, the motor has good stability and strong carrying capacity.

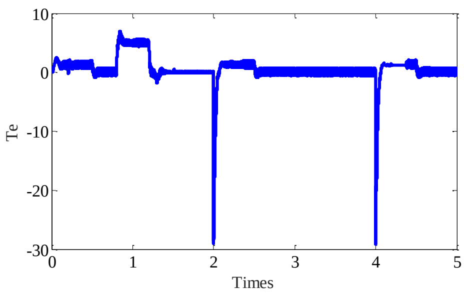

(a) Torque with time

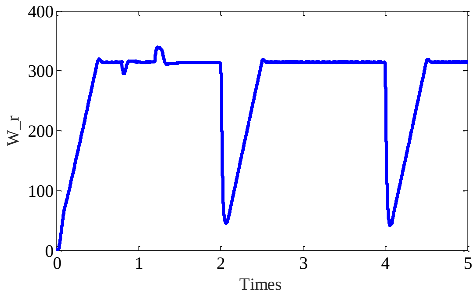

(b) Speed with time

Figure 9: Speed and curve of torque mutation.

7. CONCLUSION

The simulation results show that the speed sensorless control method of permanent magnet synchronous motor based on the estimated current model has a fast speed estimation of rotor speed. From these simulation curves, it can be found that the speed overshoot is very small and the time of reaching the stable speed is short. In each sampling period, the speed and rotor position are estimated based on the error correction between the measured current value and the estimated current value. It starts directly in the static state of the motor, has no state switching, has the fast starting ability, the high speed state runs well, and the low speed running capacity is improved significantly compared with the existing methods. The proposed algorithm is very easy to be realized through DSP, and has strong robustness to the uncertainty of motor parameters in the operation. It has the advantages of low cost, high reliability, good stability and wide range of use.

ACKNOWLEDGEMENT

This paper is funded by the Key Research and Development Plan Project of Shandong Province (NO: 2016ZDJS02A02).

REFERENCE

1. Walambe R A, Joshi V A. Closed Loop Stability of a PMSM-EKF Controller-Observer Structure [J]. IFAC-PapersOnLine, 2018; 51(1): 249-254.
2. Chen S Y, Luo Y, Pi Y G. Pmsm sensorless control with separate control strategies and smooth switch from low speed to high speed. ISA transactions, 2015; 58: 650-658.
3. Ohara M, Noguchi T. Rotor position sensorless control and its parameter sensitivity of permanent magnet motor based on model reference adaptive system. IEEJ Transactions on Industry Applications, 2012; 132: 426-436.
4. Khlaief A, Boussak M, Chaari A. A MRAS-based stator resistance and speed estimation for sensorless vector controlled IPMSM drive. Electric Power Systems Research, 2014; 108: 1-15.
5. Gao W, Guo Z. Speed sensorless control of PMSM using model reference adaptive system and RBFN[J]. Journal of networks, 2013; 8(1): 213.
6. She Zhiting, Yuan Junbo, Zheng Yong, et al. Interactive model reference adaptive PMSM speed identification. Electrical transmission, 2011; 41(3):3-7.
7. Hu Weizhen, Wang Yue, Li Mingxi, et al. Research on speed sensorless control strategy of multiphase permanent magnet direct drive wind power generation system based on MRAS. Power System Protection and Control, 2014; 23: 118-124.
8. Deng Xianming, Wang Wenwen, Pang Qingqing. Sensorless Position Detection of Permanent Magnet Synchronous Motor. Laboratory Research and Exploration, 2015; 34(4): 112-116.

9. Genduso F, Miceli R, Rando C, et al. Back EMF Sensorless-Control Algorithm for High-Dynamic Performance PMSM. IEEE Transactions on Industrial Electronics, 2010; 57(6): 2092-2100.
10. Lee G B, Park J S, Lee S H, et al. High-performance sensorless control of PMSM using back-EMF and reactive power. Iccas-Sice. IEEE, 2009; 407-411.
11. Yin Zhong-gang, Liu Jing, Zhong Yanru, et al. Low-speed performance of speed sensorless vector control for induction motor based on two-parameter model reference adaptive. Transactions of China Electrotechnical Society, 2012; 27(7): 124-130.
12. Xing Yan. Research on Key Technologies of High Performance Torque Control for Permanent Magnet Synchronous Motor. Northeastern University, 2014.
13. Lu Wenqi, Huang Wenxin, Hu Yuwen. Sensorless control of a novel sliding mode observer for permanent magnet synchronous motors. Control Theory and Applications, 2009; 26(4): 429-432.
14. Yuan Anbei. Research on Sensorless Control Technology of Permanent Magnet Synchronous Motor. Nanjing University of Science and Technology, 2014.
15. Du Lijuan, Zhang Xiaoyu. Analysis of Extended Mathematical Model of Permanent Magnet Synchronous Motor. Journal of North China University of Science and Technology, 2016.
16. Huang Chenrong, XU Bo. Simulation Analysis of Vector Control of Permanent Magnet Synchronous Motor. Electric Automation, 2016; 38(2): 11-12.
17. Xu Xinyi. Exploration of PMSM Speed Sensor Based on Extended Synovial Controller. Electronic Test, 2015; 05: 4-6.
18. Gao Zheng. Design and Implementation of PMSM Synovial Observer Based on DSP. Hangzhou Dianzi University, 2015.